Synthetic Metals 161 (2011) 2451–2459

Contents lists available at SciVerse ScienceDirect

Synthetic Metals

journal homepage: www.elsevier.com/locate/synmet

The synthesis and electroluminescent properties of dithienylquinacridone-based copolymers for white light-emitting diodes

Ho Jun Song[a], Seung Min Lee[a], Jang Yong Lee[a], Byung Hyun Choi[b], Doo Kyung Moon[a,*]

[a] Department of Material Chemistry and Engineering, Konkuk University, Seoul 143-701, Republic of Korea
[b] Electronic & Optic Materials Center, Korea Institute of Ceramic Engineering and Technology, Seoul 153-801, Republic of Korea

ARTICLE INFO

Article history:
Received 17 June 2011
Received in revised form 6 September 2011
Accepted 15 September 2011
Available online 5 October 2011

Keywords:
Conjugated polymers
PLED
Dithienylquinacridone
Fluorene

ABSTRACT

The dithienylquinacridone derivative that produces orange emission in fluorene, a representative blue light-emitting material, was added in a small quantity as a dopant to synthesize poly[fluorene-co-DTQuinacridone] (PFTQ) using the Suzuki coupling reaction. The copolymer was synthesized at various mole ratios and was soluble in organic solvents. The luminous efficiency of PFTQ3 was 0.50 cd/A, the power efficiency was 0.24 lm/W, and the maximum brightness was 1450 cd/m^2. In addition, the device made from PFTQ3 emitted white light with the CIE coordinates of (0.31, 0.35). After thermal treatment, its luminous efficiency, power efficiency and maximum brightness were 0.71 cd/A, 0.34 lm/W, and 3905 cd/m^2, respectively, corresponding to an improvement of about 1.4 times of the sample prior to thermal treatment.

1. Introduction

In the last decade, the π-conjugated polymer has been investigated for various applications including in organic light-emitting diodes (OLED) [1–5], organic thin film transistors (OTFT) [6–11], organic photovoltaic cells (OPV) [12–17]. The application that has drawn the greatest attention is its use in the organic light-emitting diode (OLED). Specially, polymer light-emitting diodes (PLED) has gained great attention as the next-generation material in the display industry because it allows manufacturing of large films through a screen printing method, compared to small molecule OLEDs that use a high vacuum deposition technique; it also enables the implementation of flexible displays due to the flexibility of the element [18–20].

Since the discovery of poly(phenylenevinylene) in 1990 [21], a number of studies have been investigated to polymer light-emitting diode materials; polyfluorene [22], poly(fluorene–phenothiazine) [23] and polycarbazole [24] as blue light-emitting materials; poly(phenylene–vinylene) [25] as green light-emitting material; poly(fluorene–thiophene) [7], poly(fluorene–benzothiophene) [26] and poly(fluorene–phenothiazine) derivatives [27] as orange and red light-emitting materials. It is possible to produce a full color display using these polymers to generate the red, green and blue (R, G, B) colors. While green and orange color elements are commercially available, blue and red light-emitting diodes have not found widespread applications [28,29].

A number of studies have also been investigated on materials that generate white emission in addition to the previous studies on red-, green- and blue-emitting materials. As a result, OLED has gained attention as a next-generation lighting source, which can replace fluorescent light and act as an alternative material for the backlight unit of LCDs [28–30]. Currently there are two methods to produce a white light-emitting material: blending RGB materials and making a single polymer. Blending RGB materials, however, results in material with low efficiency and unstable colors because of phase separation [31,32]. To resolve these issues, researchers have been investigating methods to develop elements in a single polymer system. There are two methods to produce white light-emitting materials in a single polymer system: inserting a small quantity of green and red dopants in a blue-emitting backbone [33,34], and inserting a small quantity of orange dopant in a blue backbone [35].

The fluorene derivative has been applied to white light-emitting materials in a single polymer system as a blue backbone. This is because fluorene has a high efficiency of photoluminescent (PL) quantum yield, high chemical and thermal stability, good solubility, even film formation, high molecular weight, and is easy to synthesize [36–38]. However, rigid-rod polyfluorene displays a nematic-type of arrangement due to chain aggregation as film formation. This chain aggregation reduces luminescent quantum yield. To minimize chain aggregation and maximize emission

* Corresponding author. Tel.: +82 2 450 3498; fax: +82 2 444 0765.
E-mail address: dkmoon@konkuk.ac.kr (D.K. Moon).

0379-6779/$ – see front matter © 2011 Elsevier B.V. All rights reserved.
doi:10.1016/j.synthmet.2011.09.026

efficiency, an aryl group or alkyl chain is applied to the 9-position of fluorene to enhance the performance of the fluorene derivative [39,40].

Quinacridone is chemically stable and has a high PL quantum efficiency. However, its maximum PL intensity is at 536 nm, which indicates a yellowish orange emission. When this polymer is added in a small quantity to a blue backbone, the material will emit a bluish white light. Furthermore, the effective charge trapping does not occur because the highest occupied molecular orbital (HOMO) level is 5.9 eV, which is lower than the base level of polyfluorene, which is 5.8 eV [41–46]. On the other hand, the PL spectrum of dithienylquinacridone showed a red-shift of approximately 30 nm when compared to that of the quinacridone and the HOMO level of dithienylquinacridone showed 5.46 eV. The PL spectrum was then red-shifted and the HOMO level was increased. As a result, effective charge trapping occurred as expected. However, there is no report of use of dithienylquinacridone in polymer light emitting diodes.

In this study, we synthesized the dithienylquinacridone derivative as an orange dopant. The compound poly(9,9-dioctylfluorene-co-dithienylquinacridone) (PFTQ), a new polymer enabling effective white-light emission, was synthesized using dithienylquinacridone, a novel orange chromophore, with a blue-emitting fluorene backbone at 0.01% and 0.03% molar concentration through Suzuki coupling. The oxadiazole derivative with good electron transport properties and a carbazole derivative with good hole transport properties were applied to the backbone to improve the electron and hole transporting abilities. Then, the polymers (PFoxdTQ3, PFoxdCzTQ3), which also have effective hole and electron transport properties, were synthesized with the concentration of 0.03 mol% to compare their properties.

2. Experiment

2.1. Materials and measurement

All reagents were purchased from Aldrich, Acros or TCI. All chemicals were used without further purification. The following compounds were synthesized according to modified literature procedures: 2,2′-(9,9-dioctyl-9H-fluorene-2,7-diyl)bis(4,4,5,5-tetramethyl-1,3,2-dioxaborolane) (**M3**) [5], 9-(heptadecan-9-yl)-2,7-bis(4,4,5,5-tetramethyl-1,3,2-dioxaborolan-2-yl)-9H-carbazole (**M4**) [47], 2,7-dibromo-9,9-bis(6-bromohexyl)-9H-fluorene (**M5**) [48], and 4-(5-(4-tert-butylphenyl)-1,3,4-oxadiazol-2-yl)phenol (**M6**) [49].

Unless otherwise specified, all reactions were carried out under nitrogen. Solvents were dried using standard procedures. All column chromatography was performed with the use of silica gel (230–400 mesh, Merck) as the stationary phase. ^{1}H-NMR spectra were performed in a Bruker ARX 400 spectrometer using $CDCl_3$ as the solvent and chemical shifts were recorded in units of ppm, with TMS as the internal standard. The elemental analyses were measured with EA1112 using a CE Instrument. All of the thin films were fabricated using a GMC2 spin coater (Gensys, Korea), and their thickness was measured using an alpha step 500 surface profiler (KLA-Tencor). Electronic absorption spectra were measured in chloroform using a HP Agilent 8453 UV–vis spectrophotometer. PL spectra were recorded using a Perkin Elmer LS 55 luminescence spectrometer. Cyclic voltammetry experiments were performed with a Zahner IM6eX Potentionstat/Galvanostat. All measurements were carried out at room temperature with a conventional three-electrode configuration consisting of platinum working and auxiliary electrodes and a non-aqueous Ag/AgCl reference electrode at a scan rate of 50 mV/s. The solvent in all experiments was acetonitrile and the supporting electrolyte was 0.1 M tetrabutyl ammonium-tetrafluoroborate. TGA measurements were performed on a NETZSCH TG 209 F3 thermogravimetric analyzer. All GPC analyses were made using THF as the eluant and polystyrene standard as a reference.

2.2. EL device fabrication and characterization

The fabricated device structure was ITO/PEDOT:PSS/polymer /BaF_2/Ba/Al. All of the polymer light emitting diodes were prepared using the following device fabrication procedure. The glass/indium tin oxide(ITO) substrates [Sanyo, Japan(10 Ω/γ)] were sequentially lithographically patterned, cleaned with detergent, and ultrasonicated in deionized water, acetone and isopropyl alcohol. Then the substrates were dried on a hotplate at 120 °C for 10 min and treated with oxygen plasma for 10 min in order to improve the contact angle just before the film coating process. Poly(3,4-ethylenedioxythiophene): poly(styrene-sulfonate) (PEDOT:PSS, Baytron P 4083 Bayer AG) was passed through a 0.45 μm filter before being deposited onto ITO at a thickness of ca. 32 nm through spin-coating at 4000 rpm in air and then dried at 120 °C for 20 min inside a glove box. The light-emitting polymer layer was then deposited onto the film by spin coating a polymer solution in chlorobenzene (1.5 wt.%) at a speed of 1000 rpm for 30 s on top of the PEDOT:PSS layer. The device was thermally annealed at 90 °C for 30 min in a glove box. The device fabrication was completed by depositing thin layers of BaF_2 (1 nm), Ba (2 nm) and Al (200 nm) at pressures less than 10^{-6} torr. The active area of the device was 9.0 mm^2. Finally, the cell was encapsulated using UV-curing glue (Nagase, Japan). EL spectra, Commission Internationale de l'Eclairage (CIE) coordinates, current–voltage, and brightness–voltage characteristics of devices were measured with a Spectrascan PR670 spectrophotometer at the forward direction and a computer-controlled Keithley 2400 under ambient condition.

2.3. Synthesis of monomers

2.3.1. Synthesis of 5,12-dihexylquinolino[2,3-b]acridine-7,14(5H,12H)-dione (1)

KOH (22.11 g, 160 mmol) was added to a stirred mixture of quinacridone (5 g, 16.0 mmol) in DMSO (50 mL) at room temperature. The mixture was stirred for 30 min, followed by the addition of 1-bromohexane (22.47 mL, 160 mmol). The resulting mixture was stirred for another 24 h at room temperature, and then poured into water and extracted with ethyl acetate (EA). The organic layer was washed with brine and dried over anhydrous sodium sulfate. After the solvent was removed, the crude product was purified with silica gel column using MC as the eluent. The end product had a yield of 2.90 g, or 37.7%. ^{1}H-NMR ($CDCl_3$) δ = 8.67 (s, 2H), 8.51 (d, 2H), 7.69 (t, 2H), 7.45 (d, 2H), 7.21 (t, 2H), 4.46 (t, 4H), 1.97 (m, 4H), 1.62 (m, 4H), 1.45 (m, 8H), 0.95 (m, 6H). $C_{32}H_{36}N_2O_2$: Calcd. C 79.96, H 7.55, N 5.83, O 6.66; Found C 79.96, H 7.09, N 5.77, O 6.72.

2.3.2. Synthesis of 2,9-dibromo-5,12-dihexylquinolino[2,3-b]acridine-7,14(5H,12H)-dione (M1)

A mixture of compound 1 (2 g, 4.16 mmol), CH_3COONa (0.887 g, 10.81 mmol) and acetic acid (50 mL) was heated to reflux while being stirred. A solution of Br_2 (0.495 mL, 9.56 mmol) in acetic acid (50 mL) was then added drop-wise to the mixture and stirred for 1 h. After the mixture was cooled, the precipitated solid was collected by filtration and washed with aqueous $NaHSO_3$ and water. The crude product was recrystallized from EA to give a red crystalline compound. The end product had a yield of 2.49 g, or 93.7%. ^{1}H-NMR ($CDCl_3$) δ = 8.68 (s, 2H), 8.62 (d, 2H), 7.80 (d, 2H), 7.40 (d, 2H), 7.26 (s, 2H), 4.47 (t, 4H), 1.95 (m, 4H), 1.59 (m, 4H), 1.43 (m,

8H), 0.95 (m, 6H). $C_{32}H_{34}Br_2N_2O_2$: Calcd. C 60.20, H 5.37, N 4.39, O 5.01; Found C 60.20, H 5.67, N 4.46, O 5.20.

2.3.3. Synthesis of 5,12-dihexyl-2,9-di(thiophen-2-yl)quinolino[2,3-b]acridine-7,14(5H,12H)-dione (3)

A mixture of compound 2 (1 g, 1.56 mmol), 2-(tributylstannyl) thiophene (2.33 g, 6.26 mmol), dichlorobis-(triphenylphosphine) palladium(II) (0.25 g, 0.635 mmol), DMF (10 mL) and THF (10 mL) was heated overnight under reflux. It was then cooled and the solvent was removed under reduced pressure. The product was purified with a silica gel column using EA/$CHCl_3$ as eluent. The end product had a yield of 0.23 g, or 23.7%. ^{1}H-NMR ($CDCl_3$) δ = 8.78 (d, 4H), 7.99 (d, 2H), 7.54 (d, 2H), 7.43 (s, 2H), 7.33 (d, 2H), 7.13 (d, 2H), 4.55 (t, 4H), 2.02 (m, 4H), 1.65 (m, 4H), 1.46 (m, 8H), 0.96 (m, 6H). $C_{40}H_{40}N_2O_2S_2$: Calcd. C 74.50, H 6.25, N 4.34, O 4.96, S 9.94; Found C 74.50, H 6.25, N 4.36, O 5.90, S 10.15.

2.3.4. Synthesis of 2,9-bis(5-bromothiophen-2-yl)-5,12-dihexylquinolino[2,3-b]acridine-7,14(5H,12H)-dione (M2)

Compound 3 (0.23 g, 0.37 mmol) was dissolved in $CHCl_3$ (10 mL) and acetic acid (10 mL). Subsequently, NBS (0.14 g, 0.81 mmol) was added to this solution. The mixture was heated at 40 °C for 3 h and poured into water, and then extracted with $CHCl_3$. The organic layer was washed with brine and then dried over anhydrous sodium sulfate. After removal of the solvent, the crude product was purified by recrystallization in $CHCl_3$. The yield of the end product was 0.22 g, or 77%. ^{1}H-NMR ($CDCl_3$) δ = 8.70 (d, 4H), 7.89 (d, 2H), 7.51 (d, 2H), 7.14 (d, 2H), 7.07 (d, 2H), 4.52 (t, 4H), 2.02 (m, 4H), 1.63 (m, 4H), 1.43 (m, 8H), 0.96 (m, 6H). $C_{40}H_{38}Br_2N_2O_2S_2$: Calcd. C 59.85, H 4.77, N 3.49, O 3.99, S 7.99; Found C 58.73, H 4.62, N 3.42, O 4.08, S 8.34.

2.3.5. Synthesis of 5,5′-(4,4′-(6,6′-(2,7-dibromo-9H-fluorene-9,9-diyl)bis(hexane-6,1-diyl))bis(oxy)bis(4,1-phenylene))bis(2-(4-tert-butylphenyl)-1,3,4-oxadiazole) (M7)

Compounds M5 (5.04 g, 7.763mmol) and M6 (5.03 g, 17.08 mmol) were dissolved in DMF (80 mL) and the reaction mixture stirred at 90 °C for 24 h under nitrogen. $CHCl_3$ was then added to the reaction mixture and the organic phase washed with water and brine. After drying over sodium sulfate, $CHCl_3$ was removed under reduced pressure and the crude product was purified by column chromatography over silica gel. The yield of the end product was 6.79 g, or 81%. ^{1}H-NMR ($CDCl_3$) δ = 7.96 (d, 8H), 7.46 (d, 6H), 7.39 (d, 4H), 6.88 (d 4H), 3.84 (t, 4H), 1.89 (m, 4H), 1.58 (m, 6H), 1.18 (m, 6H), 1.09 (m, 4H), 0.55 (m, 4H). $C_{61}H_{64}Br_2N_4O_4$: Calcd. C 68.03, H 5.99, N 5.20, O 5.94; Found C 67.45, H 5.97, N 5.11, O 6.25.

2.4. Polymerization

Reaction monomers $(PPh_3)_4Pd(0)$ (1.5 mol%) and Aliquat 336 were dissolved in a mixture of toluene and an aqueous solution of 2 M K_2CO_3. The solution was refluxed for 72 h with vigorous stirring under nitrogen, and an excess amount of bromobenzene, acting as the end capper, was added while the stirring continued for another 12 h. The entire mixture was then poured into methanol. The resulting precipitate was filtered off, purified with acetone and chloroform in soxhlet.

PFQ3. 9,9-dioctylfluorene-2,7-dibromofluorene (0.499 equiv.), 2,2′-(9,9-dioctyl-9H-fluorene-2,7-diyl)bis(4,4,5,5-tetramethyl-1,3,2-dioxaborolane) (M3) (0.50 equiv.), 2,9-dibromo-5,12-dihexylquinolino[2,3-b]acridine-7,14(5H,12H)-dione(M1) (0.0003 equiv.); Yield: 0.29 g (68%); ^{1}H-NMR ($CDCl_3$) δ = 7.85–7.83 (m), 7.71–7.25 (m), 2.11 (m), 1.25–1.13 (m), 0.83–0.79 (m).

PFTQ1. 9,9-dioctylfluorene-2,7-dibromofluorene (0.499 equiv.), 2,2′-(9,9-dioctyl-9H-fluorene-2,7-diyl)bis(4,4,5,5-tetramethyl-1,3,2-dioxaborolane) (M3) (0.50 equiv.), 2,9-bis(5-bromothiophen-2-yl)-5,12-dihexylquinolino[2,3-b]acridine-7,14(5H,12H)-dione (M2) (0.0001 equiv.) were used in this polymerization. Yield: 0.28 g (66%). ^{1}H-NMR ($CDCl_3$) δ = 7.85–7.83 (m), 7.71–7.25 (m), 2.11 (m), 1.25–1.13 (m), 0.83–0.79 (m).

PFTQ3. 9,9-dioctylfluorene-2,7-dibromofluorene (0.499 equiv.), 2,2′-(9,9-dioctyl-9H-fluorene-2,7-diyl)bis(4,4,5,5-tetramethyl-1,3,2-dioxaborolane) (M3) (0.50 equiv.), 2,9-bis(5-bromo thiophen-2-yl) -5,12-dihexylquinolino[2,3-b]acridine-7,14(5H,12H)-dione (M2) (0.0003 equiv.) were used in this polymerization. Yield: 0.30 g (71%). ^{1}H-NMR ($CDCl_3$) δ = 7.85–7.83 (m), 7.71–7.25 (m), 2.11 (m), 1.25–1.13 (m), 0.83–0.79 (m).

PFoxdTQ3. 5,5′-(4,4′-(6,6′-(2,7-dibromo-9H-fluorene-9,9-diyl)bis(hexane-6,1-diyl))bis(oxy)bis (4,1-phenylene))bis (2-(4-tert-butylphenyl)-1,3,4-oxadiazole) (M7) (0.499 equiv.), 2,2′-(9,9-dioctyl-9H-fluorene-2,7-diyl)bis(4,4,5,5-tetramethyl-1,3,2-dioxaborolane) (M3) (0.50 equiv.), 2,9-bis(5-bromothiophen-2-yl)-5,12-dihexylquinolino[2,3-b]acridine-7,14(5H,12H)-dione (M2) (0.0003 equiv.) were used in this polymerization. Yield: 0.49 g (36%). ^{1}H-NMR ($CDCl_3$) δ = 8.11–7.83 (m), 7.77–7.70 (m), 7.57–7.51 (m), 6.94–6.92 (m), 3.90 (O), 2.16–2.03 (m), 1.66 (m), 1.25–1.12 (m), 0.80–0.77 (m).

PFoxdCzTQ3. 5,5′-(4,4′-(6,6′-(2,7-dibromo-9H-fluorene-9,9-diyl)bis(hexane-6,1-diyl))bis (oxy)bis (4,1-phenylene))bis (2-(4-tert-butylphenyl)-1,3,4-oxadiazole) (M7) (0.499 equiv.), 9-(heptadecan-9-yl)-2,7-bis(4,4,5,5-tetramethyl-1,3,2-dioxaborolan-2-yl)-9H-carbazole (M4) (0.50 equiv.), 2,9-bis(5-bromothiophen-2-yl)-5,12-dihexylquinolino[2,3-b]acridine-7,14(5H,12H)-dione (M2) (0.0003 equiv.) were used in this polymerization. Yield: 0.55 g (41%). ^{1}H-NMR ($CDCl_3$) δ = 8.29–7.83 (m), 7.80–7.57 (m), 7.52–7.50 (m), 6.92–6.90 (m), 4.74 (N), 3.89 (O), 2.43–2.03 (m), 1.66 (m), 1.32–1.15 (m), 0.90–0.77 (m).

3. Results and discussion

3.1. Synthesis and characterization of the polymers

To compare Quinacridone of Wang and co-workers [42] and dithienylquinacridone, we synthesized polymers in same method. Polymers were synthesized by Suzuki coupling reaction according to Schemes 1 and 2, using the monomers listed. While the yield of polymers PFQ3, PFTQ1 and PFTQ3 was over 65%, the yield of polymers PFoxdTQ3 and PFoxdCzTQ3 was 36–41%. The synthesized polymers were refined by a soxhlet extractor using methanol, acetone and chloroform, in that order. The polymers dissolved well in general organic solvents including chloroform, toluene, xylene and benzene, and the films were easily made. As illustrated in Fig. 1, the ^{1}H-NMR spectrum indicates the successful synthesis of the polymer. The spectrum of the aromatic ring of the PFTQ series was observed at 7.0–8.0 ppm and the spectrum of an alkyl side chain was confirmed at 0.8–4.0 ppm. Because M1 & M2 comprised a small ratio of the total compound, its aromatic and aliphatic peaks were almost indistinguishable. According to the GPC measurement of each polymer as shown in Table 1, The number–average molecular weight (M_n) of PFQ3, PFTQ1, PFTQ3, PFoxdTQ3 and PFoxdCzTQ3 were relatively high: 23,700, 13,600, 14,600, 13,300 and 15,000, respectively. Polydispersity indices (PDIs) of these polymers were 2.03, 1.93, 2.19, 2.07 and 2.00, respectively. The thermal properties of the polymers were measured by TGA. Polymers PFQ3, PFTQ1, PFTQ3, PFoxdTQ3 and PFoxdCzTQ3

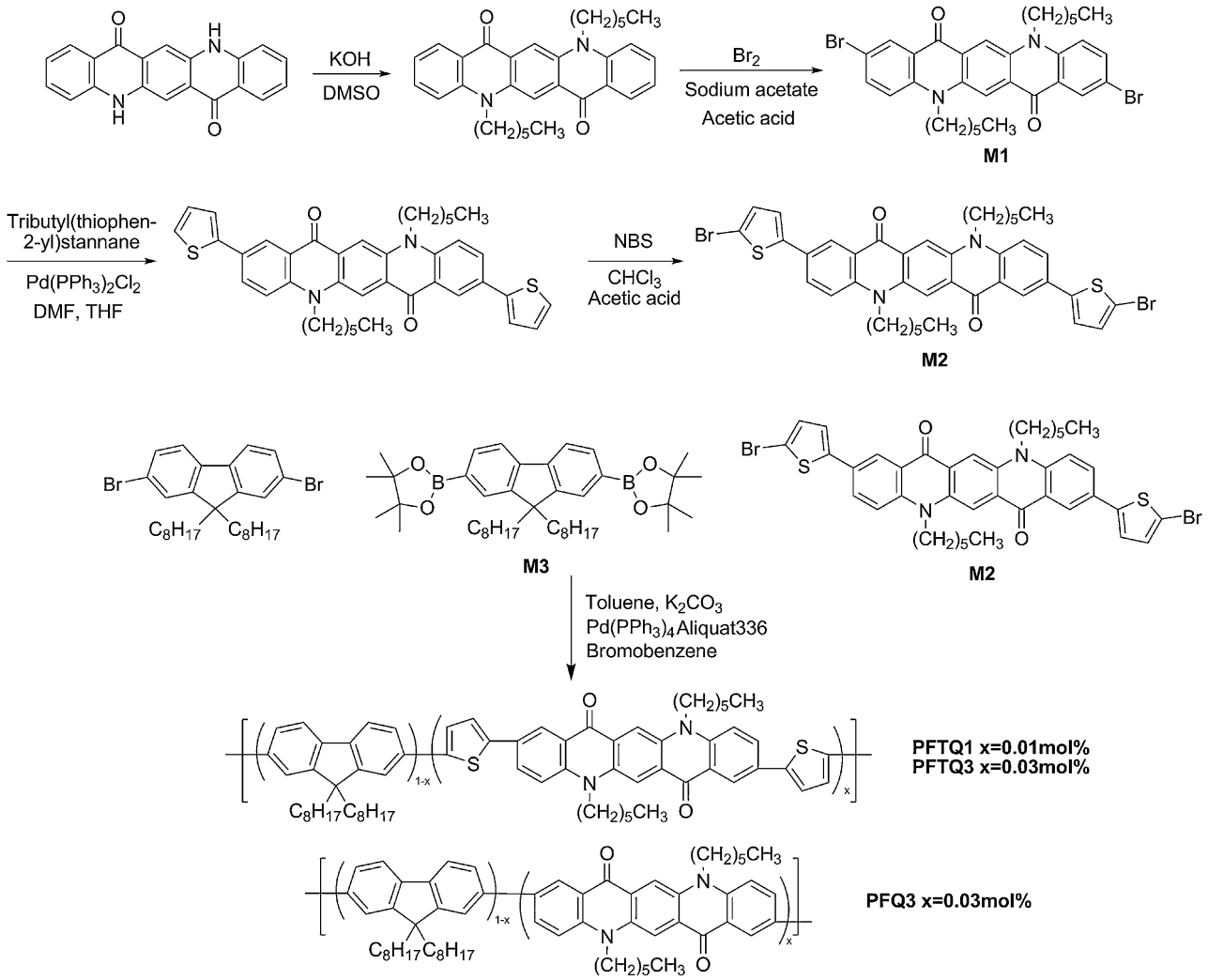

Scheme 1. Synthesis of monomers and polymerization of PFQ3, PFTQ1, PFTQ3.

had 5% weight loss at the temperatures of 358, 423, 413, 416 and 424 °C, respectively, displaying high thermal stability. Thus, it is estimated that the polymers will be stable during the manufacturing or operation process of a device at high temperatures.

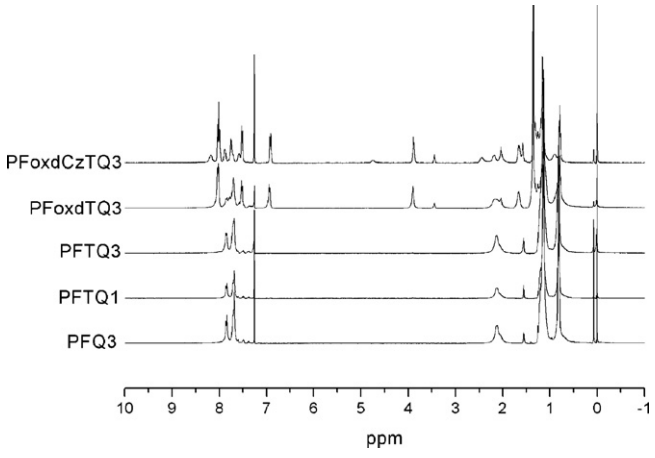

Fig. 1. ^{1}H-NMR spectra of polymers.

3.2. Optical and electrochemical properties

The UV–vis absorption spectra and PL spectra of the polymers were investigated both in chlorobenzene and as films cast from solution. Figs. 2 and 3 display the absorption and photoluminescence (PL) spectra of the polymers in dilute solution (5 μg/mL) and thin film (thickness: 80 nm). The absorption peaks for PFQ3, PFTQ1 and PFTQ3 in solution were located at 384, 386 and 385 nm, respectively, while maxima absorption peaks for all of polymers showed 382 nm in film, similar to the spectrum of polyfluorene. The absorption bands of the dithienylquinacridone derivative were not observed at 510 and 545 nm due to its low concentration. Polymers PFoxdTQ3 and PFoxdCzTQ3 also showed nearly the same spectra, with another absorption band appearing around 300 nm because of the oxadiazole moiety. PFoxdCzTQ3 showed broader absorption spectrum in the range from 250 nm to 300 nm than that of

Table 1
Physical and thermal properties.

Polymer	M_n	M_w	PDI	T_d(°C)
PFQ3	23,700	48,200	2.03	358
PFTQ1	13,600	26,300	1.93	423
PFTQ3	14,600	32,000	2.19	413
PFoxdTQ3	13,300	27,600	2.07	416
PFoxdCzTQ3	15,000	30,000	2.00	424

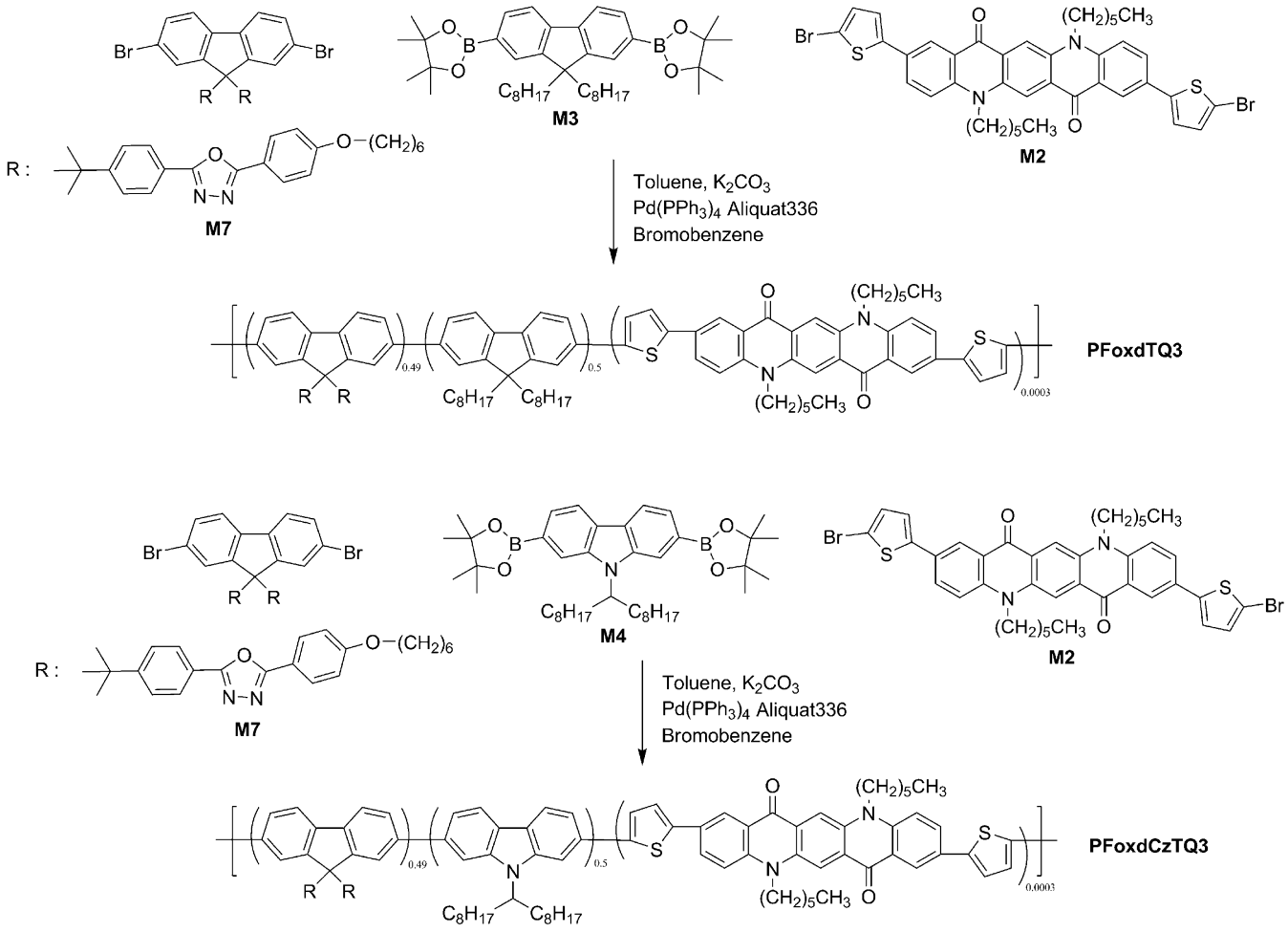

Scheme 2. Polymerization of PFoxdTQ3, PFoxdCzTQ3.

PFoxdTQ3 due to the effect of the carbazole derivative. The film cast showed nearly the same results. The maximum absorption peak position of the film displayed a blue-shift of about 2–3 nm compared to the solution, which may be caused by π–π stacking. The optical band gap energy between the HOMO level and the lowest unoccupied molecular orbital (LUMO) level was obtained using the onset value of the absorption spectrum. Since the onset values of PFQ3, PFTQ1, PFTQ3, PFoxdTQ3 and PFoxdCzTQ3 absorption spectra were similar, the band gap energy of the polymers was 3.00 eV.

The maxima of the PL spectra of PFQ3, PFTQ1, PFTQ3, PFoxdTQ3 and PFoxdCzTQ3 in a solution state were similarly observed at 417 nm, while their maxima in the film state differed. For PFQ3, PFTQ1 and PFTQ3 as films, the maxima of the PL spectra were observed at 437 nm, and the shoulder peaks of PFQ3, PFTQ1 and PFTQ3 were found at 462 and 540 nm, 462 and 557 nm, 464 and 558 nm, respectively. The PFQ3 peak observed around 540 nm was due to quinacridone, whereas the PFTQ1 and PFTQ3 peaks observed around 557 nm were due to dithienylquinacridone. Compared to PFQ3, Both PFTQ1 and PFTQ3 showed red-shifted PL spectrum of 17 nm, it originated from extended conjugated length by segment of thiophene. The maxima of the PL spectra of PFoxdTQ3 and PFoxdCzTQ3 were at 425 and 428 nm, respectively, which showed a blue-shift by about 8–11 nm compared to PFTQ1 and PFTQ3. This result may be due to the ultraviolet-blue light emission from the oxadiazole and carbazole derivative [46].

As shown in Fig. 4, the absorption spectrum of dithienylquinacridone overlapped with the PL spectrum of polyfluorene. This phenomenon indicates that the effective Forster energy transfer is expected from the fluorene segment to the dithienylquinacridone derivative (M2). Furthermore, the PL spectrum of the dithienylquinacridone derivative showed a red-shift of approximately 30 nm when compared to the spectrum of the quinacridone derivative (M1). This is a result of the extended π-conjugation of quinacridone by the thiophene group in the main chain.

Fig. 5 describes the HOMO and LUMO levels acquired using the onset values of cyclic voltammetry [50]. The scan rate of cyclic voltammetry was set at 50 mV/s and the reference electrode was Ag/AgCl. The HOMO value was calculated using the Eq. (1) after compensation using ferrocene:

$$\mathrm{HOMO(eV)} = -4.8 - (E_{\mathrm{onset}} - E_{1/2}(\mathrm{Ferrocene})) \quad (1)$$

As a result, the PFQ3, PFTQ1, PFTQ3, PFoxdTQ3 and PFoxdCzTQ3 HOMO levels were 5.77, 5.77, 5.77, 5.73 and 5.71 eV, respectively. However, the LUMO level was barely observable using cyclic voltammetry. Thus the LUMO values were obtained using the optical band gap acquired by UV absorption in the HOMO level above, which were 2.77, 2.77, 2.77, 2.73 and 2.71 eV, respectively. PFoxdTQ3 and PFoxdCzTQ3 had a little high HOMO levels, it originated from the oxadiazole and carbazole derivatives. This indicates that hole injection may be more effective compared with PFTQ1 and PFTQ3. Moreover, as shown in the energy level diagram in Fig. 5, the HOMO level of dithienylquinacridone (M2) was 5.46 eV and the LUMO level was 3.31 eV, whereas the HOMO level of quinacridone (M1) was 5.76 eV and the LUMO level was 3.37 eV.

Table 2
Optical and electrochemical properties of polymers.

Polymer	Solution		Film		E_{HOMO} (eV)	E_{LUMO}[a] (eV)
	Absorption	Emission	Absorption	Emission		
PFQ3	384	418, 440	386	437, 462, 540	5.77	2.77
PFTQ1	386	417, 441	382	438, 462, 557	5.77	2.77
PFTQ3	385	417, 440	382	438, 464, 558	5.77	2.77
PFoxdTQ3	300, 385	417, 441	300, 383	425, 449, 558	5.73	2.73
PFoxdCzTQ3	300, 390	417, 441	299, 387	428, 450, 559	5.71	2.71

[a] $E_{LUMO} = E_{HOMO} - E_{optical\ band\ gap}$.

It is expected that charge trapping from the fluorene segment to dithienylquinacridone may be more effective than that from the fluorene segment to quinacridone [33,42]. Table 2 summarizes the optical and electrochemical properties.

3.3. Electroluminescence properties and current–voltage–luminance characteristics

Fig. 6 shows the electroluminescence properties of the PFTQ series. The structure of the single light-emitting diode (LED) was made as ITO/PEDOT:PSS/polymer/BaF_2/Ba/Al. The polymer, which was the active layer, was about 70 nm thick and was made using a spin-coating method. The turn-on voltage of the device made for this study was 5 V. The EL emission spectrum of the polymer was generally broad, which was slightly different from

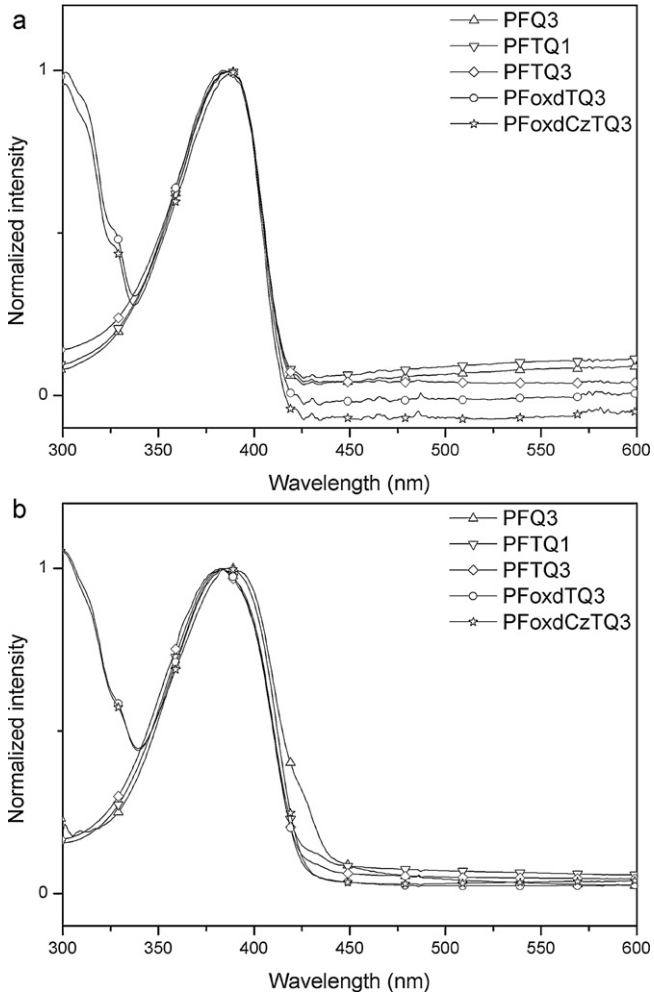

Fig. 2. UV–vis absorption spectrum (a) in solution (5 μg/mL) and (b) in thin film (thickness: 80 nm) of the PFTQ series.

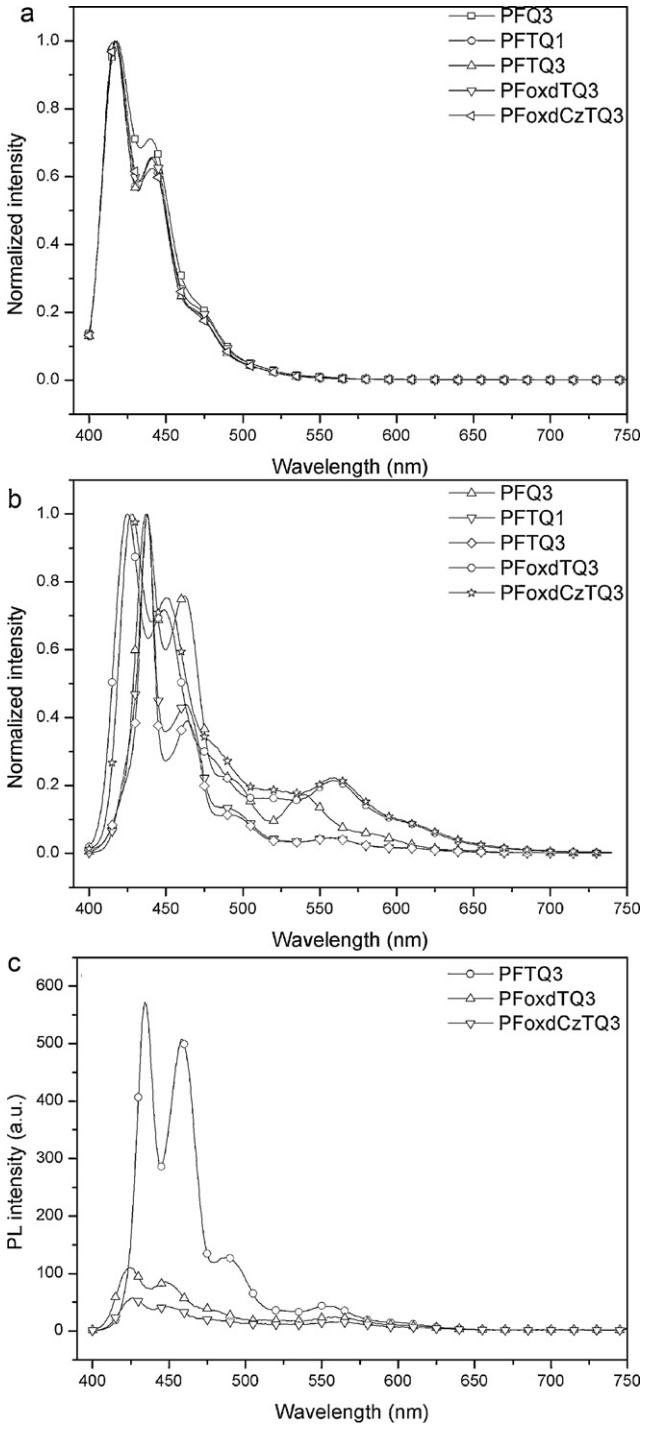

Fig. 3. Normalized PL emission spectrum (a) in solution (5 μg/mL) (b) in thin film (thickness: 80 nm) of the PFTQ series and (c) PL spectrum intensities of PFTQ3, PFoxdTQ3, PFoxdCzTQ3 in the same thickness (80 nm).

Table 3
Summary of EL device performances of the PFTQ series.

Polymer	EL emission λ_{max}	Luminous efficiency (cd/A)	Power efficiency (lm/W)	Maximum brightness (cd/m^2)	EQE (%)	CIE coordinates (x,y)
PFQ3	434, 462, 490, 540	0.41 (0.52)[a]	0.19 (0.23)[a]	1757 (3825)[a]	0.10 (0.18)[a]	(0.23, 0.29) (0.21, 0.26)[a]
PFTQ1	434, 462, 494, 556	0.38 (0.83)[a]	0.19 (0.34)[a]	1805 (3011)[a]	0.14 (0.33)[a]	(0.28, 0.34) (0.23, 0.25)[a]
PFTQ3	434, 462, 492, 558	0.50 (0.71)[a]	0.24 (0.34)[a]	1450 (3905)[a]	0.12 (0.25)[a]	(0.31, 0.35) (0.26, 0.29)[a]
PFoxdTQ3	426, 452, 562	0.31 (0.40)[a]	0.14 (0.21)[a]	763 (1437)[a]	0.11 (0.13)[a]	(0.28, 0.29) (0.28, 0.29)[a]
PFoxdCzTQ3	428, 452, 562	0.34 (0.21)[a]	0.18 (0.09)[a]	1106 (1628)[a]	0.11 (0.07)[a]	(0.31, 0.34) (0.30, 0.34)[a]

[a] EL performance after thermal treatment at 120 °C for 10 min.

the PL spectrum. It is estimated that the charge trapping of dithienylquinacridone had an impact on the results above. The polymer showed strong emission peaks at 430, 460 and 560 nm. The peaks around 430 and 460 nm originated from fluorene, oxadiazole and carbazole derivatives. The peak around 560 nm was caused by the dithienylquinacridone derivative. PFoxdTQ3 and PFoxdCzTQ3 had broader peaks around 500 nm compared to PFTQ1 and PFTQ3, which was likely to be caused by the π–π aggregation of the oxadiazole derivative. PFQ3 and PFTQ1 showed bright blue color emissions, whereas PFTQ3, PFoxdTQ3 and PFoxdCzTQ3 showed white color emission. In particular, the PFTQ3 polymer with CIE coordinates of (0.31, 0.35) was close to pure white light with the coordinates (0.33, 0.33) suggesting that PFTQ3 had the best performance among all polymers. The luminous efficiency, power efficiency and maximum brightness of PFTQ3 were 0.50 cd/A, 0.24 lm/W, and 1450 cd/m^2, respectively. The properties of PFTQ3 were superior to that of PFQ3 because charge trapping was more effective in dithienylquinacridone compared to quinacridone. Device structure of Wang group is ITO/PEDOT:PSS/polymer/Ca/Al. On the other hand, Our device structure is ITO/PEDOT:PSS/polymer/BaF_2/Ba/Al. The structure of device had a big effect on CIE coordinate and power conversion efficiency [51]. As a result, it showed different result compared to result of Wang group. Therefore, we fabricated device of PFQ3 and PFTQ3 in the same conditions to demonstrate excellent properties of PFTQ3 compared to PFQ3. As shown in Table 3, EQE value of PFTQ3 was superior to that of PFQ3 because charge trapping was more effective in dithienylquinacridone compared to quinacridone. Contrary to what was expected, the properties of PFoxdTQ3 and PFoxdCzTQ3 were not superior to the properties of PFTQ3 despite their pure white emissions. This is because charge transportation was hindered by the dominant shielding effect of the fluorene backbone of the oxadiazole derivative [52]. Therefore, it is expected that effective transport properties can be acquired by adjusting the mole ratio of the oxadiazole derivative to less than 50 mol%. To demonstrate shielding effect, photoluminescence spectra of PFTQ3, PFoxdTQ3, PFoxdCzTQ3 were investigated as films cast (thickness: 80 nm) in the same condition. As shown in Fig. 3(c), it showed that PL intensities of PFoxdTQ3, PFoxdCzTQ3 were much lower compared to that of PFTQ3, which implies oxadiazole derivative exhibit dominant shielding effect of fluorene backbone. Thus, as other work, we believe that these electroluminescence characteristics could be further improved by reduction of dominant shielding effect and efficient electron injection through introducing small ratio of oxadiazole derivative. [53,54].

A number of studies aimed at improving the performance of devices using thermal treatment have been conducted because thermal treatment improves the interfacial adhesion between

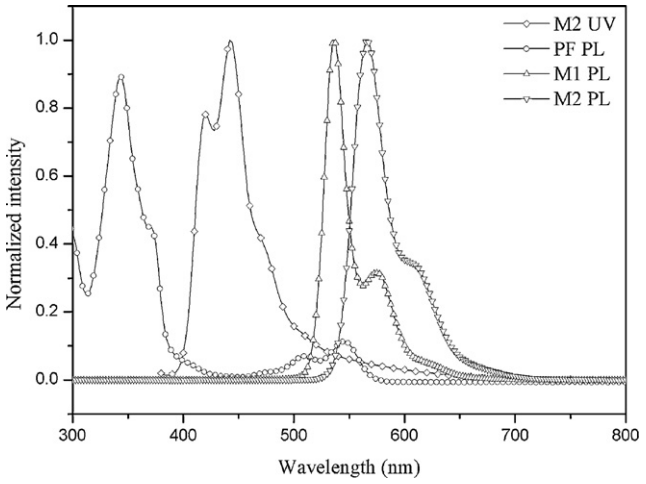

Fig. 4. UV–vis absorption spectrum of M2 and PL emission spectrum of PF, M1, M2.

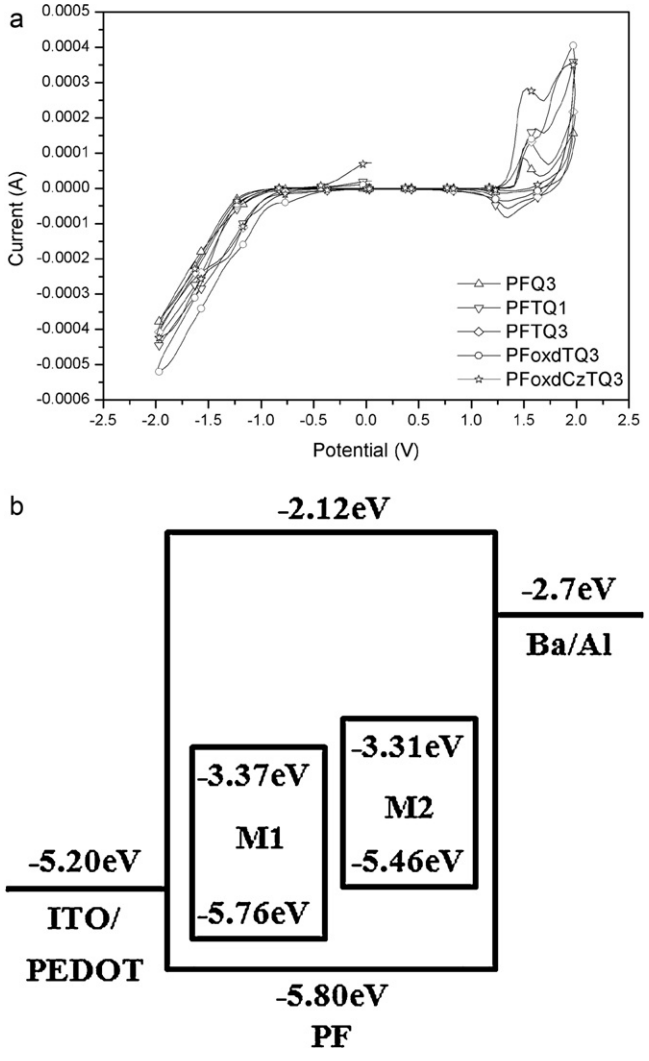

Fig. 5. (a) Cyclic voltammograms of polymers. (b) The energy levels of PF, M1 and M2.

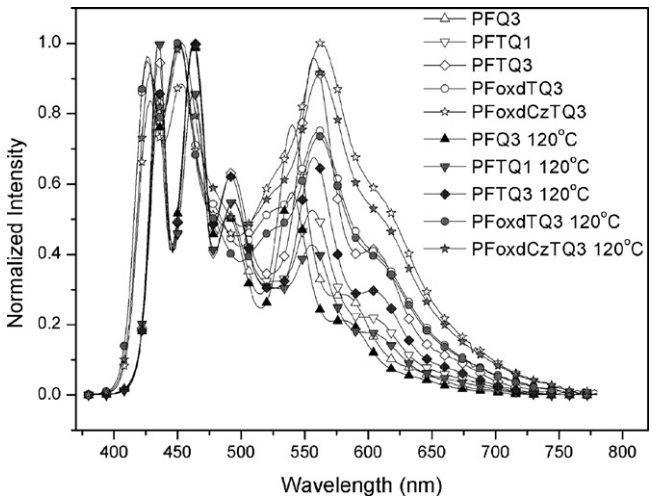

Fig. 6. EL luminescence spectrum of the PFTQ series.

emissive layers and cathodes, and it also increases contact area [34,55]. Thus, the device properties were evaluated after thermal treatment at 120 °C for 10 min, as shown in Table 3. The luminous efficiency, power efficiency and maximum brightness of PFTQ1 and PFTQ3 were 0.83 and 0.71 cd/A, 0.34 and 0.34 lm/W, and 3011 and 3905 cd/m^2, respectively. The results after thermal treatment were improved by about 1.4 to 2.1 times compared to results prior to thermal treatment. As mentioned above, this is because the interfacial adhesion improved and contact area increased. After annealing, CIE coordinates of PFQ3, PFTQ1, PFTQ3 were blue-shifted to (0.21, 0.26), (0.23, 0.25), and (0.26, 0.29), respectively. It can be seen that annealing the active layer at above 120 °C reinforces the blue emission obviously. The increased blue emission peaks are caused by crystalline α-phase PF emission in active films [56,57]. The voltage–luminance (*V–L*), current density–luminous efficiency (*J–LE*) curve and properties of the device are summarized in Fig. 7 and Table 3.

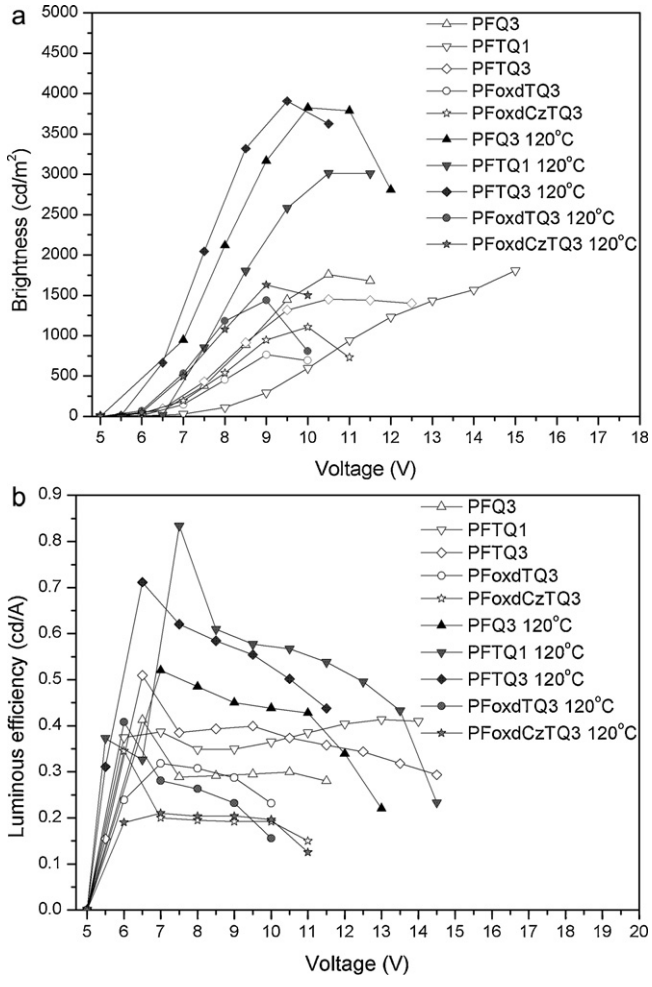

Fig. 7. (a) Voltage–luminance (*V–L*) curve. (b) Current density–luminous efficiency (*J–LE*) curve.

4. Conclusions

In this study, a new white-emitting polymer was successfully synthesized by applying dithienylquinacridone, which is a novel orange-emitting chromophore, onto a fluorene (blue-emitting chromophore) backbone. The synthesized PFTQ polymer series showed good solubility and thermal stability. The emission peaks in the EL emission spectrum were generally broader than those in the PL emission spectrum due to charge trapping of the dopant. The PFTQ3 polymer presented the best properties among all polymers studied, with luminous efficiency, power efficiency and maximum brightness values of 0.50 cd/A, 0.24 lm/W, and 1450 cd/m^2, respectively. Its CIE coordinates (0.31, 0.35) were close to pure white. After thermal treatment, the luminous efficiency, power efficiency and maximum brightness of PFTQ3 were evaluated and found to be 0.71 cd/A, 0.34 lm/W, and 3905 cd/m^2, respectively, due to the improvement of interfacial adhesion and increase of contact area. The results after thermal treatment were improved by about 1.4–2.1-fold compared to prior to thermal treatment. In conclusion, the realization of white light emission using a blue chromophore and a novel orange chromophore was verified.

Acknowledgments

This work was supported by the Energy Efficiency & Resources of the Korea Institute of Energy Technology Evaluation and Planning(KETEP) grant funded by the Korea government Ministry of Knowledge Economy.

References

[1] R.H. Friend, R.W. Gymer, A.B. Holmes, J.H. Burroughes, R.N. Marks, C. Taliani, D.D.C. Bradley, D.A. Dos Santos, J.L. Bredas, M. Logdlund, W.R. Salaneck, Nature 397 (1999) 121–128.
[2] P. Rungta, V. Tsyalkovsky, C.F. Huebner, Y.P. Bandera, S.H. Foulger, Synth. Met. 160 (2010) 2486–2493.
[3] W. Lu, J. Kuwabara, T. Kanbara, Macromolecules 44 (2011) 1252–1255.
[4] H.J. Song, J.Y. Lee, I.S. Song, D.K. Moon, J.R. Haw, J. Ind. Eng. Chem. 17 (2011) 352–357.
[5] J.Y. Lee, M.H. Choi, D.K. Moon, J.R. Haw, J. Ind. Eng. Chem. 16 (2010) 395–400.
[6] B.L. Lee, T. Yamamoto, Macromolecules 32 (1999) 1375–1385.
[7] I. Mcculloch, M. Heeney, C. Bailey, K. Genevicius, I. Macdonald, M. Shkunov, D. Sparrowe, S. Tierney, R. Wagner, W. Zhang, M.L. Chabinyc, R.J. Kline, M.D. Mcgehee, M.F. Toney, Nat. Mater. 5 (2006) 328–333.
[8] T. Yasuda, T. Imase, T. Yamamoto, Macromolecules 38 (2005) 7378–7385.
[9] A. Tanimoto, T. Yamamoto, Macromolecules 39 (2006) 3546–3552.
[10] S. Samitsu, Y. Takanishi, J. Yamamoto, Macromolecules 42 (2009) 4366–4368.
[11] G. Lu, H. Usta, C. Risko, L. Wang, A. Facchetti, M.A. Ratner, T.J. Marks, J. Am. Chem. Soc. 130 (2008) 7670–7685.
[12] V. Tamilavan, M.K. Song, S.H. Jin, M.H. Hyun, J. Polym. Sci. Part A: Polym. Chem. 48 (2010) 5514–5521.
[13] J.Y. Lee, M.H. Choi, H.J. Song, D.K. Moon, J. Polym. Sci. Part A: Polym. Chem. 48 (2010) 4875–4883.
[14] J.Y. Lee, S.W. Heo, H.L. Choi, Y.J. Kwon, J.R. Haw, D.K. Moon, Sol. Energy Mater. Sol. Cells 93 (2009) 1932–1938.
[15] J.Y. Lee, W.S. Shin, J.R. Haw, D.K. Moon, J. Mater. Chem. 19 (2009) 4938–4945.
[16] F.C. Krebs, Sol. Energy Mater. Sol. Cells 93 (2009) 465–475.
[17] C.M. MacNeill, E.D. Peterson, R.E. Noftle, D.L. Carroll, R.C. Coffin, Synth. Met. 161 (2011) 1137–1140.
[18] G. Gustafsson, Y.T. Cao, G.M. Klavetter, F. Colaneri, A.J. Heeger, Nature 357 (1992) 477–479.

[19] A.J. Heeger, Solid State Commun. 107 (1998) 673–679.
[20] M.M. Alam, S.A. Jenekhe, Chem. Mater. 14 (2002) 4775–4780.
[21] J.H. Burroughes, D.D.C. Bradley, A.R. Brown, R.N. Marks, K. Mackay, R.H. Friend, P.L. Burns, A.B. Holmes, Nature 347 (1990) 539–541.
[22] Q. Pei, Y. Yang, J. Am. Chem. Soc. 118 (1996) 7416–7417.
[23] D.H. Hwang, S.K. Kim, M.J. Park, J.H. Lee, B.W. Koo, I.N. Kang, S.H. Kim, T.Y. Zyung, Chem. Mater. 16 (2004) 1298–1303.
[24] A. Iraqi, I. Wataru, Chem. Mater. 16 (2004) 442–448.
[25] Z. Tan, R. Tang, E. Zhou, Y. He, C. Yang, F. Xi, Y. Li, Adv. Polym. Sci. 107 (2008) 514–521.
[26] Q. Hou, Y. Xu, W. Yang, M. Yuan, J. Peng, Y. Cao, J. Mater. Chem. 12 (2002) 2887–2892.
[27] M.J. Park, J.H. Lee, I.H. Jung, J.H. Park, D.H. Hwang, H.K. Shim, Macromolecules 41 (2008) 9643–9649.
[28] B.W. D'Andrade, S.R. Forrest, Adv. Mater. 16 (2004) 1585–1595.
[29] S.K. Lee, T. Ahn, N.S. Cho, J.I. Lee, Y.K. Jung, J.H. Lee, H.K. Shim, J. Polym. Sci. Part A: Polym. Chem. 45 (2007) 1199–1209.
[30] M. Berggren, O. Inganas, G. Gustasson, J. Rasmusson, M.R. Andersson, T. Hjerberg, W. Wennerstrom, Nature 372 (1994) 444–446.
[31] S. Tasch, E.J.W. List, C. Hockfilzer, G. Leising, P. Schlichting, U. Rohr, Y. Geerts, U. Scherf, K. Mullen, Phys. Rev. 56 (1997) 4479–4483.
[32] S. Tasch, E.J.W. List, O. Ekstrom, W. Graupner, G. Leising, P. Schlichting, U. Rohr, Y. Geerts, U. Scherf, K. Mullen, Appl. Phys. Lett. 71 (1997) 2883–2885.
[33] J. Liu, Z. Xie, Y. Cheng, Y. Geng, L. Wang, X. Jing, F. Wang, Adv. Mater. 19 (2007) 531–535.
[34] J. Luo, X. Li, Q. Hou, J. Peng, W. Yang, Y. Cao, Adv. Mater. 19 (2007) 1113–1117.
[35] J. Liu, Y. Cheng, Z. Xie, Y. Geng, L. Wang, X. Jing, F. Wang, Adv. Mater. 20 (2008) 1357–1362.
[36] M. Grell, X. Long, D.D.C. Bradely, M. Inbasekaran, F.P. Woo, Adv. Mater. 9 (1997) 798–802.
[37] N.S. Cho, D.H. Hwang, J.I. Lee, B.J. Jung, H.K. Shim, Macromolecules 35 (2002) 1224–1228.
[38] A. Charas, J. Morgado, J.M.G. Martinho, L. Alcácer, S.F. Lim, R.H. Friend, F. Cacialli, Polymer 44 (2003) 1843–1850.
[39] S. Setayesh, A.C. Grimsdale, T. Weil, V. Enkelmann, K. Mullen, F. Meghdadi, E.F.W. List, G. Leising, J. Am. Chem. Soc. 123 (2001) 946–953.
[40] M.R. Craig, M.M.D. Kok, J.W. Hofstraat, A.P.H.J. Schenning, E.W. Meijer, J. Mater. Chem. 13 (2003) 2861–2862.
[41] J. Wang, Y. Zhao, C. Dou, H. Sun, P. Xu, K. Ye, J. Zhang, S. Jiang, F. Li, Y. Wang, J. Phys. Chem. B 111 (2007) 5082–5089.
[42] J. Liu, B. Gao, Y. Cheng, Z. Xie, Y. Geng, L. Wang, X. Jing, F. Wang, Macromolecules 41 (2008) 1162–1167.
[43] Y. Zhao, X. Mu, C. Bao, Y. Fan, J. Zhang, Y. Wang, Langmuir 25 (2009) 3264–3270.
[44] J. Shi, C.W. Tang, Appl. Phys. Lett. 70 (1997) 1665–1667.
[45] S.E. Shaheen, G.E. Jabbour, B. Kippelen, N. Peyghambarian, Appl. Phys. Lett. 74 (1999) 3212–3214.
[46] K. Ye, J. Wang, H. Sun, Y. Liu, Z. Mu, F. Li, S. Jiang, J. Zhang, H. Zhang, Y. Wang, C.M. Che, J. Phys. Chem. B 109 (2005) 8008–8016.
[47] N. Blouin, A. Michaud, M. Leclerc, Adv. Mater. 19 (2007) 2295–2300.
[48] S.H. Oh, S.I. Na, Y.C. Nah, D.J. Vak, S.S. Kim, D.Y. Kim, Org. Electron. 8 (2007) 773–783.
[49] Y.G. Jin, J.Y. Kim, S.H. Park, J.W. Kim, S.G. Lee, K.H. Lee, H.S. Suh, Polymer 46 (2005) 12158–12165.
[50] D.K. Moon, M. Ezuka, T. Maruyama, K. Osakada, T. Yamamoto, Macromolecules 26 (1993) 364–369.
[51] H.Y. Chen, C.T. Chen, C.T. Chen, Macromolecules 43 (2010) 3613–3623.
[52] C.W. Wu, C.M. Tsai, H.C. Lin, Macromolecules 39 (2006) 4298–4305.
[53] F. Huang, Y. Zhang, M.S. Liu, Y.J. Cheng, K.Y. Jen, Adv. Funct. Mater. 17 (2007) 3808–3815.
[54] C.H. Chien, P.I.C.F.S.H.U. Shih, J. Polym. Sci. Part A: Polym. Chem. 45 (2007) 2938–2946.
[55] X. Guo, C. Qin, Y. Cheng, Z. Xie, Y. Geng, X. Jing, F. Wang, L. Wang, Adv. Mater. 21 (2009) 3682–3688.
[56] B. Zhang, C. Qin, J. Ding, L. Chen, Z. Xie, Y. Cheng, L. Wang, Adv. Funct. Mater. 20 (2010) 2951–2957.
[57] S.H. Chen, A.C. Su, C.H. Su, Macromolecules 38 (2005) 379–385.